

Proton spin relaxation induced by quantum tunneling in Fe8 molecular nanomagnet

Miki Ueda and Satoru Maegawa

Graduate School of Human and Environmental Studies, Kyoto University, Kyoto 606-8501, Japan

Susumu Kitagawa

Faculty of Engineering, Kyoto University, Kyoto 606-8501, Japan

(Received 19 April 2002; published 26 August 2002)

The spin-lattice relaxation rate T_1^{-1} and NMR spectra of ^1H in single crystal of molecular magnets Fe8 have been measured down to 15 mK. The relaxation rate T_1^{-1} shows a strong temperature dependence down to 400 mK. The relaxation is well explained in terms of the thermal transition of the iron state between the discrete energy levels of the total spin $S=10$. The relaxation time T_1 becomes temperature independent below 300 mK and is longer than 100 s. In this temperature region stepwise recovery of the ^1H -NMR signal after saturation was observed depending on the return field of the sweep field. This phenomenon is attributed to the resonant quantum tunneling at the fields where levels cross and is discussed in terms of the Landau-Zener transition.

DOI: 10.1103/PhysRevB.66.073309

PACS number(s): 76.60.-k, 75.45.+j

Recently, molecular nanomagnets have attracted much attention to study quantum mechanical phenomena in the macroscopic system owing to their identical size, the well-defined structure and a well-characterized energy structure.¹⁻³ The molecular magnet $[(\text{C}_6\text{H}_{15}\text{N}_3)_6\text{Fe}_8\text{O}_2(\text{OH})_{12}]\text{Br}_7(\text{H}_2\text{O})\text{Br}\cdot 8\text{H}_2\text{O}$, abbreviated Fe8, is a representative compound in which quantum tunneling of magnetization (QTM) has been observed as the temperature-independent recovery of magnetization below 400 mK.⁴⁻⁷

The molecular magnet Fe8 consists of eight Fe^{3+} ions with spin $s=5/2$ in each molecule. The magnetic interactions between the spins in the molecule are antiferromagnetic and their magnitudes are 22–170 K,⁸ while the magnetic interactions between the molecules are negligibly small. The magnetic properties of this compound at low temperatures have been described by a total spin of $S=10$ for each molecule, in which six spins are parallel to each other and the remaining two spins are antiparallel to the six spins.^{8,9} The spin Hamiltonian in the field \mathbf{H} is expressed by

$$\mathcal{H} = DS_z^2 + E(S_x^2 - S_y^2) + g\mu_B \mathbf{S} \cdot \mathbf{H}, \quad (1)$$

where D and E are the easy axis and the in-plane anisotropy, respectively.⁴ We have determined the values of $D = -0.276$ K and $E = -0.035$ K by magnetization measurement on a single crystal.⁹ When there is no magnetic field, the anisotropy stabilizes the degenerate spin states of $m = \pm 10$ at low temperatures. These states correspond to opposite directions of the magnetization in the classical sense. The energy barrier caused by the anisotropy for reversal of the magnetization between $m = \pm 10$ is reported to be 25 K.⁴

Quantum tunneling of magnetization in Fe8 has been observed only by magnetization measurements.⁴⁻⁷ In order to study the spin dynamics in Fe8 from a microscopic point of view we performed NMR experiments and found a stepwise recovery of the ^1H spin echo signal due to resonant quantum tunneling at the level crossing fields.

We synthesized single crystals of Fe8, following the method reported previously.¹⁰ The sizes of the crystals used

for the experiments were about $4 \times 2 \times 1$ mm³. The NMR spectrum and the spin-lattice relaxation rate T_1^{-1} of ^1H in Fe8 were measured by the coherent pulsed NMR method in external magnetic fields up to 5.4 T. The spectra were obtained by measuring the spin-echo intensity with sweeping the field at a fixed frequency. The relaxation rate was obtained by measuring the recovery of the spin echo intensity as a function of the time after saturation of the ^1H spins using comb pulses. The experimental temperature was lowered down to 15 mK using a ^3He - ^4He dilution refrigerator. The samples were sealed with ^4He gas in a cell made of PCTFE plastic (polychlorotrifluoroethylene). The cell was set in the mixing chamber of the dilution refrigerator.

The NMR spectrum at room temperature is narrow with the width smaller than 50 Oe, while the spectrum becomes broader and shows structure at lower temperatures. The structure is caused by freezing of the iron magnetization and the existence of many ^1H sites.

Figure 1 shows the temperature dependence of the relaxation rate T_1^{-1} . The rate T_1^{-1} decreases steeply over six decades with lowering the temperature from 10 K to 400 mK, and decreases with increasing field. Below 300 mK T_1^{-1} is almost temperature independent and has a strong site dependence, as is found in Fig. 1.

Figure 2 shows NMR spectra of the single crystal at 150 mK. The field was applied so as to make an angle θ of 50° from the easy axis and to be within the ab plane. In this experiment we first saturated the ^1H spin system by the comb pulses at a fixed frequency, sweeping the field up and down between 0.1 and 1.5 T for more than three times, until there was no observation of the echo signals. Then the field was decreased to a certain field H_r , with a constant sweep rate dH/dt . Immediately after arriving at H_r , the field was increased with the same sweep rate and the spectrum was taken at a fixed repetition time. No signals were expected to be observed, because the returning duration after the saturation was planned to be enough shorter than the relaxation time that is longer than 100 s. Indeed no signals except from

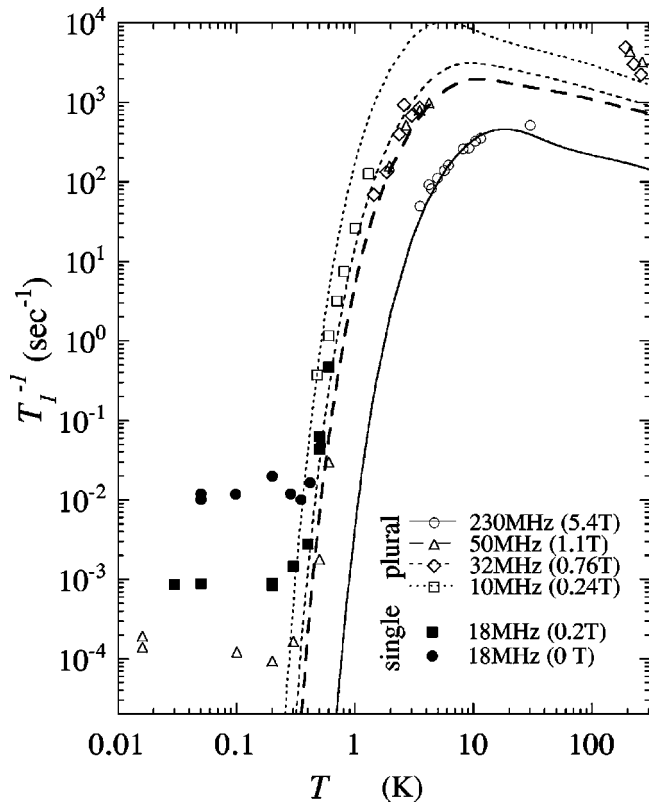


FIG. 1. Temperature dependence of relaxation rate T_1^{-1} for the samples composed of plural single crystals and for a single crystal. Lines denote calculated values.

^{19}F in the material of the sample cell and ^3He in the mixing chamber were observed when the field was returned at 0.05 T, as shown in the lowest spectrum in Fig. 2. However, signals were observed when the return fields were negative.

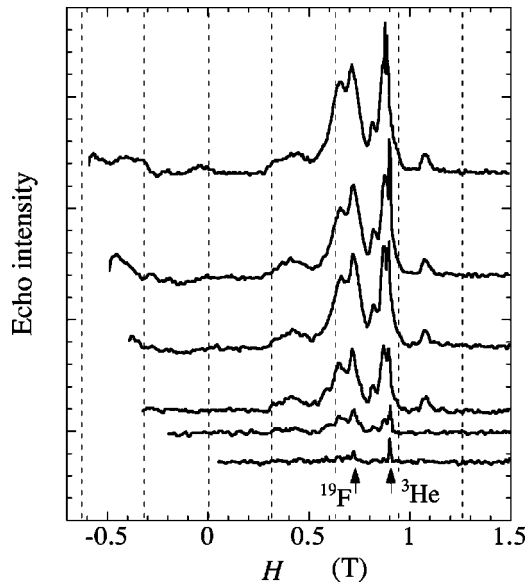


FIG. 2. NMR spectra of single crystal Fe8, which were taken with increasing the field from H_r after the saturation. $T = 150$ mK, $f = 29$ MHz, $dH/dt = 0.9$ T/min, and $\theta = 50^\circ$. Broken lines show the level crossing fields.

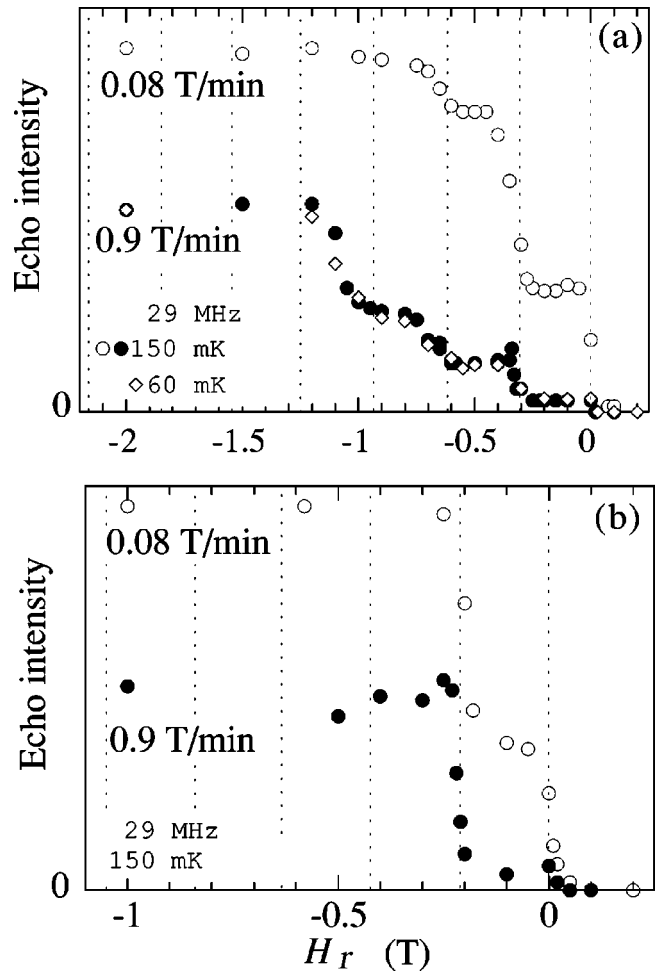


FIG. 3. Return field H_r dependence of echo intensity at field of (a) 0.45 T, $\theta = 50^\circ$ and (b) 0.60 T, $\theta = 0^\circ$. Broken lines show calculated level crossing fields. The echo intensity at 60 mK in (a) is normalized with that for 150 mK at $H_r = -2.0$ T.

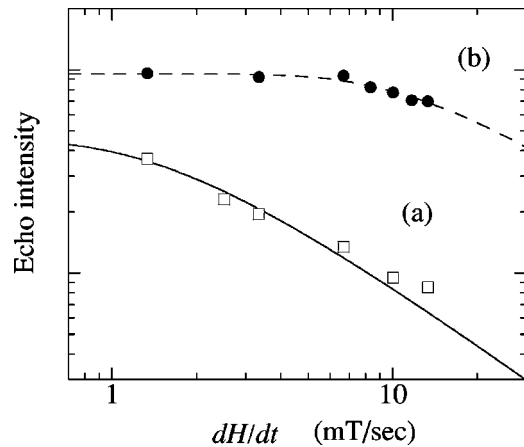


FIG. 4. Sweep rate dH/dt dependence of echo intensity at 0.60 T when (a) $H_r = -0.1$ T and (b) $H_r = -0.3$ T. The field is applied parallel to the easy axis. The solid and broken lines show calculated values by Eqs. (8) and (9), respectively.

The intensities of the signals increased with decreasing return field.

Figures 3(a) and 3(b) show the return field dependence of the echo intensity. Figure 3(a) was obtained in the case when the field was applied with $\theta=50^\circ$ within the ab plane. Figure 3(b) is the case when the field was parallel to the easy axis ($\theta=0^\circ$). The echo intensities were picked up at fields of 0.45 and 0.60 T for Figs. 3(a) and 3(b), respectively. The intensity increases sharply with steps at 0, -0.31 , -0.63 , and -1.00 T for Fig. 3(a), while for Fig. 3(b) the steps are at $+0.02$ and -0.20 T. The increase in the intensity at the steps cannot be explained by recovery due to the spin-lattice relaxation time shown in Fig. 1. Moreover the intensity is dependent on the sweep rate of the field, but independent on temperature. Figure 4 shows the sweep rate dependence of the intensity at a field of 0.60 T when the field was applied parallel to the easy axis and the return fields were -0.1 T and -0.3 T. The intensity is large when the sweep rate is slow.

First we analyze the relaxation rate. The temperature dependent relaxation rates of a molecular magnet Mn12 were first discussed by Lascialfari *et al.*¹¹ In general T_1^{-1} is given by the Fourier transform of the correlation function for fluctuating transverse local fields $h_\pm(t)$ at nuclear sites, and is expressed as

$$\frac{1}{T_1} = \frac{\gamma_N^2}{2} \int \langle \{h_\pm(t)h_\mp(0)\} \rangle e^{i\omega_L t} dt, \quad (2)$$

where γ_N is the nuclear gyromagnetic ratio and ω_L is the Larmor frequency. When the correlation is assumed to be described by an exponential function with a lifetime τ_m in the m state, the correlation can be expressed as

$$\langle \{h_\pm(t)h_\mp(0)\} \rangle = \sum_{m=-10}^{+10} \langle \Delta h_\pm^2 \rangle e^{-t/\tau_m} \frac{e^{-E_m/k_B T}}{Z}, \quad (3)$$

where E_m is the energy of the eigenstate m and Z is the partition function. The lifetime τ_m for the m state is governed by the spin-phonon interaction \mathcal{H}_{sp} and is expressed by the probabilities $p_{m \rightarrow m-1}$ for the transition from the m to the $m-1$ state and $p_{m \rightarrow m+1}$ for that from the m to the $m+1$ state, as follows:¹²

$$\frac{1}{\tau_m} = p_{m \rightarrow m-1} + p_{m \rightarrow m+1} = \begin{cases} \frac{C\Delta E_m^3}{e^{\Delta E_m/k_B T} - 1} + \frac{C\Delta E_{m+1}^3}{1 - e^{-\Delta E_{m+1}/k_B T}} & (\text{for } m > 0), \\ \frac{C\Delta E_m^3}{1 - e^{-\Delta E_m/k_B T}} + \frac{C\Delta E_{m+1}^3}{e^{\Delta E_{m+1}/k_B T} - 1} & (\text{for } m < 0), \end{cases} \quad (4)$$

where $\Delta E_m = |E_{m-1} - E_m|$. The parameter C is given by

$$C = \frac{3}{2\pi\rho v^5 \hbar^4} |\langle m | \mathcal{H}_{sp} | m \pm 1 \rangle|^2, \quad (5)$$

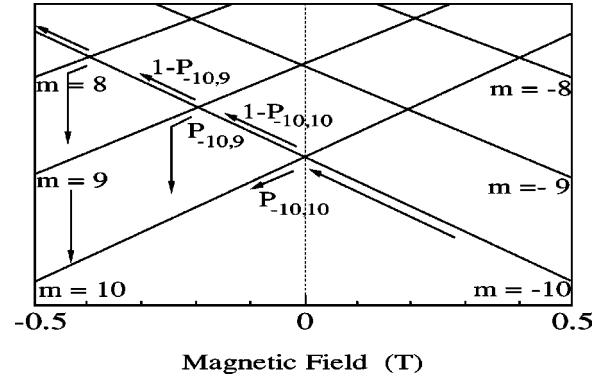


FIG. 5. Schematic energy level diagram of the spin system and the transitions.

where v is the phonon velocity and ρ is the specific mass. Thus the spin-lattice relaxation rate is obtained as

$$\frac{1}{T_1} = \frac{A}{Z} \sum_{m=-10}^{+10} \frac{\tau_m e^{-E_m/k_B T}}{1 + \omega_L^2 \tau_m^2}, \quad (6)$$

where $A = \gamma_N^2 \langle \Delta h_\pm^2 \rangle$.

The relaxation rates calculated by using Eq. (6) with fitting parameters $A = 4 \times 10^{12}$ rad/s² and $C = 5 \times 10^5$ Hz/K³ are shown for several fields in Fig. 1. The experimental results of the temperature and field dependence above 400 mK are well reproduced over six decades by this calculation. This means that relaxation above 400 mK is dominated by thermal fluctuations resulting from the transitions of iron spins between neighboring states due to spin-phonon interactions. The deviations at high temperatures must be caused by the contribution from higher energy levels which are not described by the simplified spin model with $S=10$.

The observed T_1^{-1} below 300 mK deviates from the calculated values and becomes temperature independent. This may be related to the temperature independent recovery of magnetization that has been observed in SQUID below 400 mK at nonlevel crossing fields,⁴ and may be attributed to the quantum effect.

Next we discuss the stepwise behavior of the echo intensity, shown in Fig. 3. Figure 5 shows schematically the field dependence of the energy levels of the iron spin system described by Eq. (1) and the transitions of the states when the field is decreased. In the experiment, when the field is positive at low temperatures, all the spins are in the $m=-10$ state. When the field is decreased to zero, the level of the $m=-10$ state crosses with that of the $m=10$ state, and the spins in the $m=-10$ state would change to the $m=10$ state by quantum tunneling with a probability $P_{-10,10}$. Further decrease of the field causes the energy levels to cross again and the transition to occur again. The transition at the point where the levels cross has been calculated by Landau and Zener, and the probability from the m state to the m' state in this case is expressed¹³⁻¹⁵ as

$$P_{m,m'} = 1 - \exp\left(-\frac{\pi \Delta_{m,m'}^2}{2\hbar g \mu_B |m-m'| dH/dt}\right), \quad (7)$$

where $\Delta_{m,m'}$ is the tunneling gap at the level crossing. These transitions would induce fluctuations of the local field at proton sites and cause extra relaxation of the nuclear spins.

After quantum tunneling, the spin state rapidly relaxes to the lower energy levels, following the Boltzmann distribution. The lifetime τ_m below 300 mK estimated is to be less than 10^{-7} sec from the measured relaxation time and Eq. (6). It should be noted that these thermal transitions can occur only between states with the same sign of m , while quantum tunneling occurs between states with opposite sign of m .

The measured period of the stepwise behavior for $\theta=50^\circ$ was 0.32 T, while that for $\theta=0^\circ$ was 0.22 T. The period of level crossing fields is expressed approximately as $\Delta H = D/g\mu_B \cos \theta$ and the values are 0.31 and 0.21 T for $\theta=50^\circ$ and 0° , respectively. The values coincide fairly well with the experimental results. These results clearly indicate that the sudden recovery of the ^1H spins is caused by resonant quantum tunneling of the iron magnetization at the level crossing fields.

When the iron spin state in a certain molecule changes through tunneling, the ^1H spins in the molecule would be rapidly relaxed. The iron spins which have tunneled in zero or negative fields arrive at the $m=10$ state and have possibility to tunnel again in the zero or positive fields. If it is assumed that the iron spins which have experienced tunneling once at least contribute to the proton relaxation, the echo intensities I_i at the monitoring field after the field returning would be expressed as

$$I_1 = I_{01} \{1 - (1 - P_{-10,10})^2\}, \quad (8)$$

for $H_{-10,9} < H_r < 0$, and

$$I_2 = I_{02} \{1 - (1 - P_{-10,10})^2 (1 - P_{-10,9})^2\}, \quad (9)$$

for $H_{-10,8} < H_r < H_{-10,9}$, where $H_{m,m'}$ is the crossing field of the states m and m' . The measured sweep rate dependence of echo intensities was fitted to Eqs. (8) and (9) with Eq. (7), $\Delta_{-10,10} = 3.52 \times 10^{-7}$ K and $\Delta_{-10,9} = 9.66 \times 10^{-7}$ K, as shown in Fig. 4. The agreement between calculated and ex-

perimental values is reasonably good and these values for $\Delta_{-10,10}$ and $\Delta_{-10,9}$ are close to those reported from magnetization measurements.^{6,7}

As is found in Fig. 3(b), the echo intensities for $H_r < -0.25$ T at a sweep rate of 0.9 T/min remain constant and smaller than those for $dH/dt = 0.08$ T/min. The stepwise recovery was not observed for the lower crossing fields. An intensity of the signals which were measured at the slow sweep rate of 0.08 T/min with H_r less than -0.6 T corresponds to the intensity of the signal which recovered completely. This intensity was obtained for the fast rate of 0.9 T/min by sweeping the field up and down three times between -0.1 and -0.6 T. However, the intensity after sweeping up and down three times at lower fields between -0.6 and -1.0 T with $dH/dt = 0.9$ T/min remained small. This suggests that tunneling does not occur at fields lower than -0.6 T, though the reason is not clear.

In conclusion, the proton relaxation rate T_1^{-1} of Fe8 above 400 mK is dominated by the thermal fluctuation of the iron magnetization with spin $S=10$. The transition of magnetization between the states split by DS_z^2 is caused by the spin-phonon interaction, and induces the fluctuation at nuclear sites. The rate becomes temperature independent below 300 mK. In this temperature region the stepwise recovery of the echo intensity caused by quantum tunneling at the level crossing fields was observed in the ^1H -NMR spectrum. This indicates that the internal field at proton sites fluctuates due to the resonant quantum tunneling of iron spins, which is described by the Landau-Zener transition. The temperature independent relaxation rates themselves measured below 300 mK are governed by the temperature independent correlation times possibly related to the quantum effect, however, this quantum process is another one than the resonant quantum tunneling.

We would like to thank Prof. S. Miyashita and Dr. K. Saito for valuable discussions. We also thank Dr. H. Miyasaka and Dr. H. -C. Chang for their helpful advice on synthesis of the samples.

¹D. Gatteschi, A. Caneschi, L. Pardi, and R. Sessoli, *Science* **265**, 1054 (1994).

²L. Thomas, F. Lionti, R. Ballou, D. Gatteschi, R. Sessoli, and B. Barbara, *Nature (London)* **383**, 145 (1996).

³J. R. Friedman, M. P. Sarachik, J. Tejada, and R. Ziolo, *Phys. Rev. Lett.* **76**, 3830 (1996).

⁴C. Sangregorio, T. Ohm, C. Paulsen, R. Sessoli, and D. Gatteschi, *Phys. Rev. Lett.* **78**, 4645 (1997).

⁵T. Ohm, C. Sangregorio, and C. Paulsen, *J. Low Temp. Phys.* **113**, 1141 (1998).

⁶W. Wernsdorfer, R. Sessoli, A. Caneschi, D. Gatteschi, and A. Cornia, *Europhys. Lett.* **50**, 552 (2000).

⁷W. Wernsdorfer and R. Sessoli, *Science* **284**, 133 (1999).

⁸C. Delfs, D. Gatteschi, L. Pardi, R. Sessoli, K. Wieghardt, and D. Hanke, *Inorg. Chem.* **32**, 3099 (1993).

⁹M. Ueda, S. Maegawa, H. Miyasaka, and S. Kitagawa, *J. Phys. Soc. Jpn.* **70**, 3084 (2001).

¹⁰K. Wieghardt, K. Pohl, I. Jibril, and G. Huttner, *Angew. Chem. Int. Ed. Engl.* **23**, 77 (1984).

¹¹A. Lascialfari, Z.H. Jang, F. Borsa, P. Carretta, and D. Gatteschi, *Phys. Rev. Lett.* **81**, 3773 (1998).

¹²J. Villain, F. H-Boutron, R. Sessoli, and A. Rettori, *Europhys. Lett.* **27**, 159 (1994).

¹³L. Landau, *Phys. Z. Sowjetunion* **2**, 46 (1932).

¹⁴C. Zener, *Proc. R. Soc. London, Ser. A* **137**, 696 (1932).

¹⁵S. Miyashita, *J. Phys. Soc. Jpn.* **64**, 3207 (1995).